

# ALMA Memo No. 409

February 20, 2002

## Test Report of the Baseline ALMA Correlator Digital Filter

Ray Escoffier and Jim Pisano  
National Radio Astronomy Observatory  
Charlottesville, VA 22903, USA

**Abstract:** The results of tests run on the prototype digital filter printed circuit card intended for the ALMA correlator are presented. Passband performance of the filter for all ALMA modes, as well as stop band operation for selected modes, is documented.

**Keywords:** correlator, digital filter

### INTRODUCTION

The prototype digital FIR filter logic card designed for the baseline ALMA correlator has been tested using a test fixture, and test results are presented here. All testing was done using digitally-generated signal simulations as input drive to the filter card. The filter has not yet been tested using actual digitized analog signals as will be used with the card in actual operation.

Two previous reports have been published giving the results of filter card testing. Copies of these test reports are available on the web at

[http://www.alma.nrao.edu/development/correlator/Alma\\_Correlator\\_Filter\\_Card\\_Test\\_Report.pdf](http://www.alma.nrao.edu/development/correlator/Alma_Correlator_Filter_Card_Test_Report.pdf)

and

[http://www.alma.nrao.edu/development/correlator/ALMA\\_Corr\\_Filter\\_Card\\_Test\\_Report2.pdf](http://www.alma.nrao.edu/development/correlator/ALMA_Corr_Filter_Card_Test_Report2.pdf)

The first report describes testing of the filter card to verify logical operation. The second report presents the results of testing the filter card being used as an actual digital filter with simulated input drive signals.

This memo contains much of the information originally presented in the second report, together with the results of additional measurements of the filter out-of-band rejection performance.

### TEST SET-UP

All performance results presented in this memo were obtained using a test fixture designed to test the filter and station cards of the baseline ALMA correlator. This test fixture simulated digitized analog drive signals using EXOR feedback pseudorandom number (PN) generators for the simulation of wideband noise and digital number controlled oscillators (NCOs) for the simulation of narrow spectral features. The "frequency" and "intensity" of the NCO outputs were programmable.

No attempt was made to insure that drive signals to the filter card had Gaussian amplitude distributions.

The filter card was tested using simulations of both 4-bit, 16-level and 3-bit, 8-level samples.

The test fixture used RAM buffers to drive the filter card at the full specification of 4-GS/S sample rate even though the test fixture operated with only a 125 MHz clock rate. The test setup is seen in Figure 1.

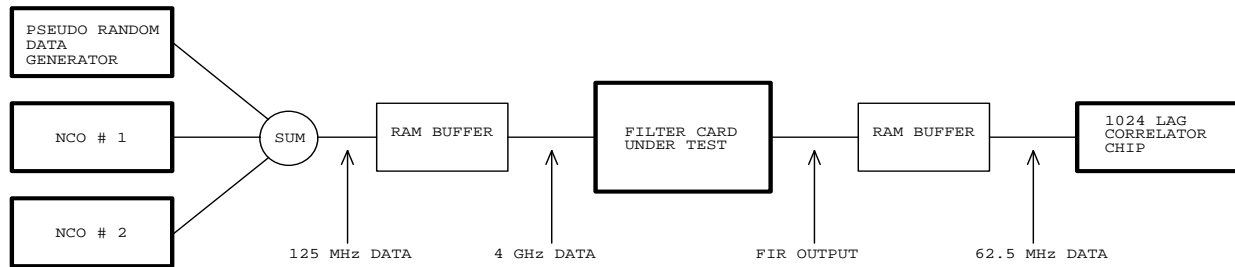


Fig. 1. Text fixture signal path.

Operation of the test fixture was bursty in nature. The input RAM buffer was filled with simulated samples derived from the PN generator and NCO outputs at the 125 MHz test fixture clock rate. This RAM buffer would then deliver a 4- $\mu$ sec packet of "samples" to drive the filter card input at an aggregate 4 GHz data rate over 32 parallel 4-bit or 3-bit wide interface lines into the filter card under test.

Filter card output samples from 4 GHz to 125 MHz, depending on the filter card decimation factor, were then written into a second test fixture RAM buffer for subsequent analysis using a (2-bit, 3-level) 1024-lag GBT correlator chip working with a 62.5 MHz clock.

## PASS BAND TESTING

Pass band testing of the prototype filter card was performed in each of the five ALMA operating modes going in binary steps from a 128-tap, 1/2 band filter to a 2048-tap, 1/32 band filter. For each operating mode, four different filter designs were tested:

1. a sharp cutoff filter with 0.95 band efficiency
2. a more gentle cutoff filter with 0.9 band efficiency
3. a partial band filter with a 0.75 band cutoff
4. a bandpass filter

(Band efficiency above is defined in terms of the useable amount of the passband selected. For example, a 1/2 band filter with a 0.95 band efficiency had a designed 3 dB point at 0.95 GHz, so the useable output extends in frequency from 0 to 0.95 GHz.)

All pass band test results of the digital filter shown in this memo were done using 4-bit samples; however, no significant differences in the pass band filter shapes are observed when 3-bit samples are used.

In Figures 2 (A and B) through 21 (A and B) below, performance in each of the five filter modes is described in a set of eight figures, two for each of the different filter designs listed above. For 1/2 band operation of the filter, for example, Figures 2A, 3A, 4A, and 5A give the predicted filter performance as calculated by the filter design software, while Figures 2B, 3B, 4B, and 5B give corresponding actual prototype filter card performance as measured in the test fixture. Since the filter card output is always Nyquist sampled, only the pass band can be seen in the actual performance figures.

In the partial band and bandpass filters, a floor 20 to 25 dB below the pass band signal is seen. This attenuation level is not a measure of the filter rejection in the stop band, but is only the correction level of the quantization correction for the 3-level GBT correlator chip. As mentioned above, the quantization correction used was not strictly correct because of the non-Gaussian nature of the signals.

Fig. 2A. 1/2 band filter design with 0.95 band efficiency.

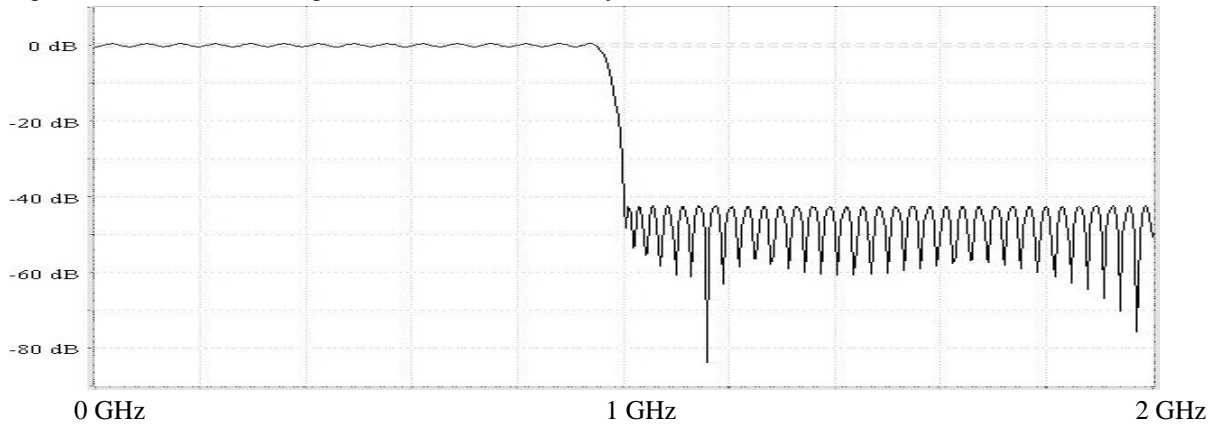


Fig. 2B. 1/2 band filter performance.

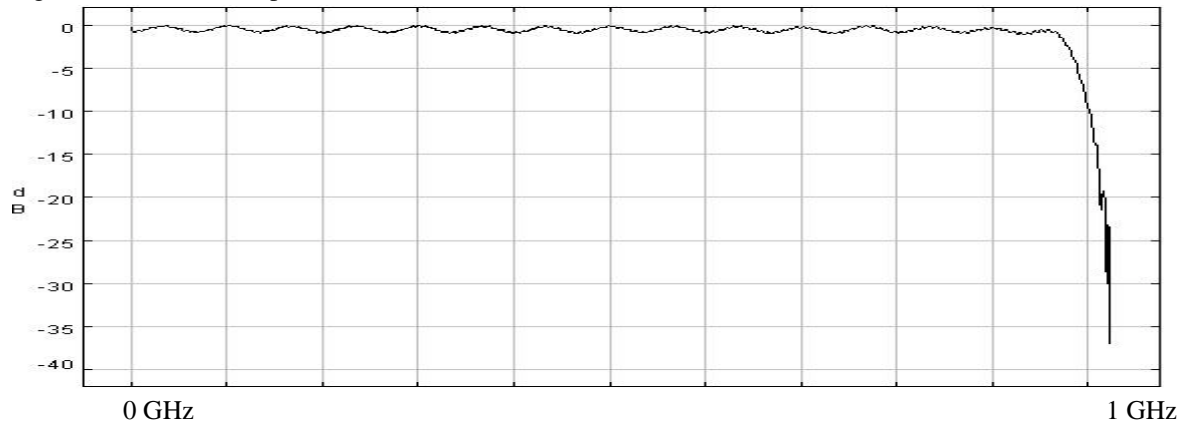


Fig. 3A. 1/2 band filter design with 0.9 band efficiency.

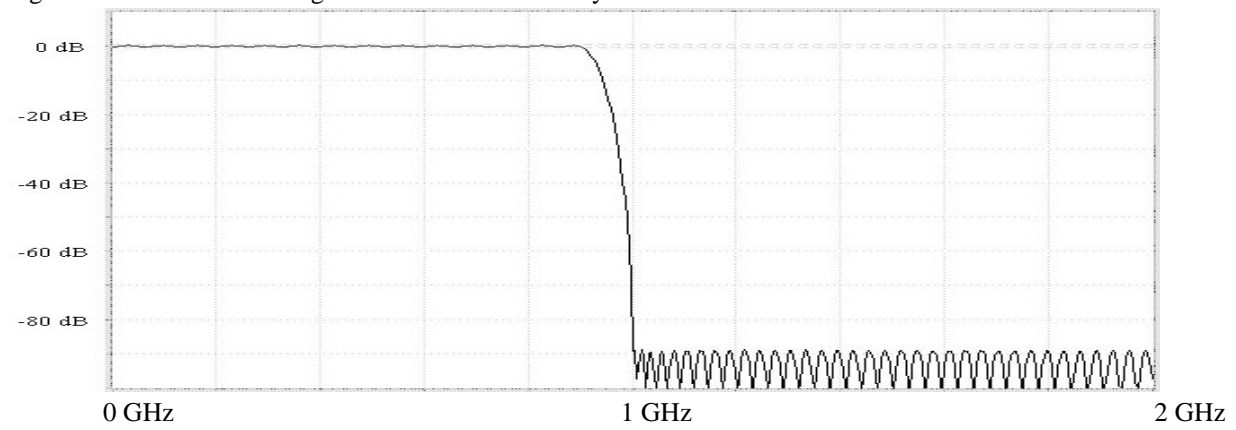


Fig. 3B. 1/2 band filter performance.

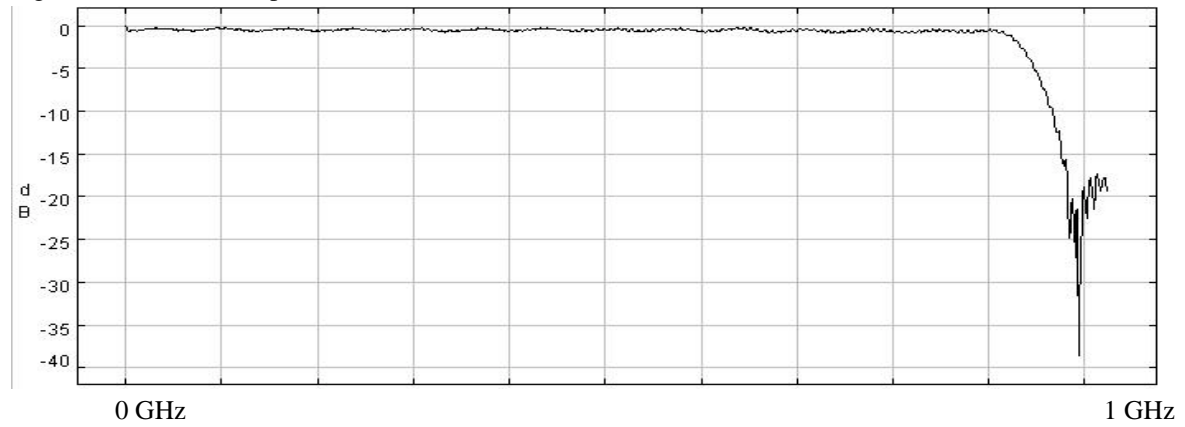


Fig. 4A. 1/2 band filter design with 0.75 band efficiency.

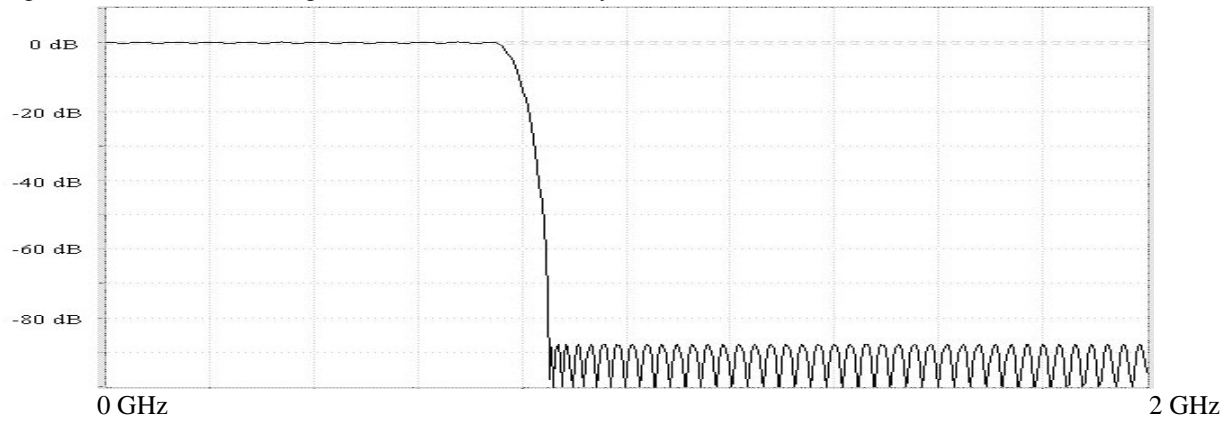


Fig. 4B. 1/2 band filter performance.

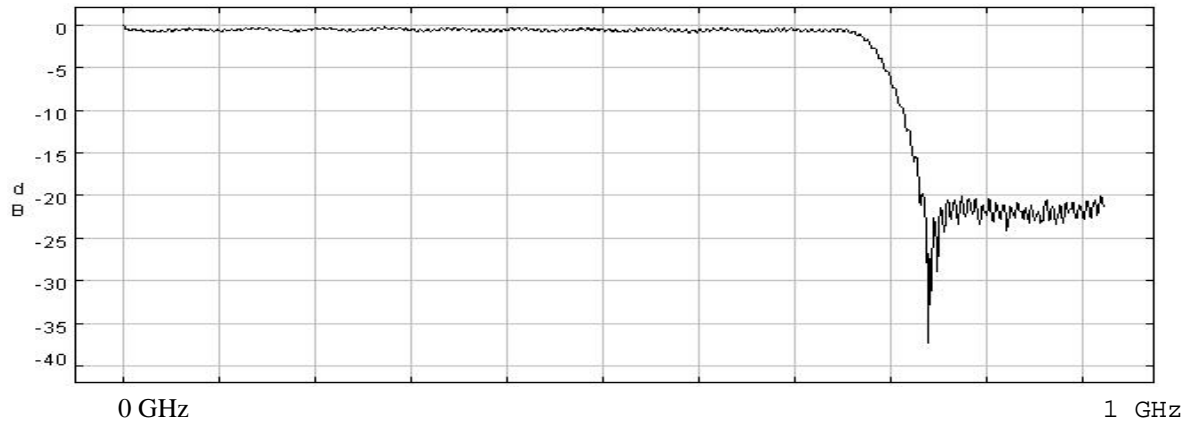


Fig. 5A. 1/2 band filter design (band pass).

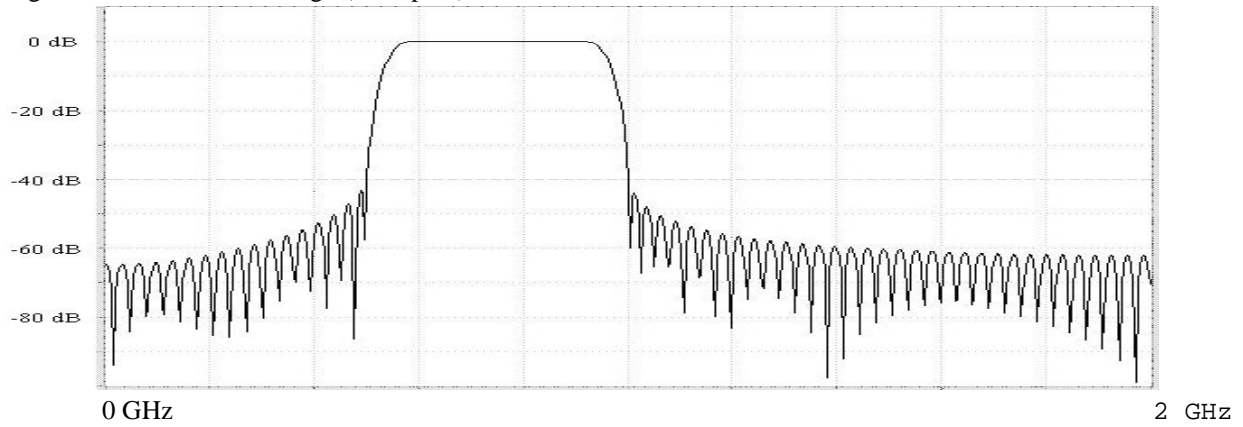


Fig. 5B. Bandpass filter performance.

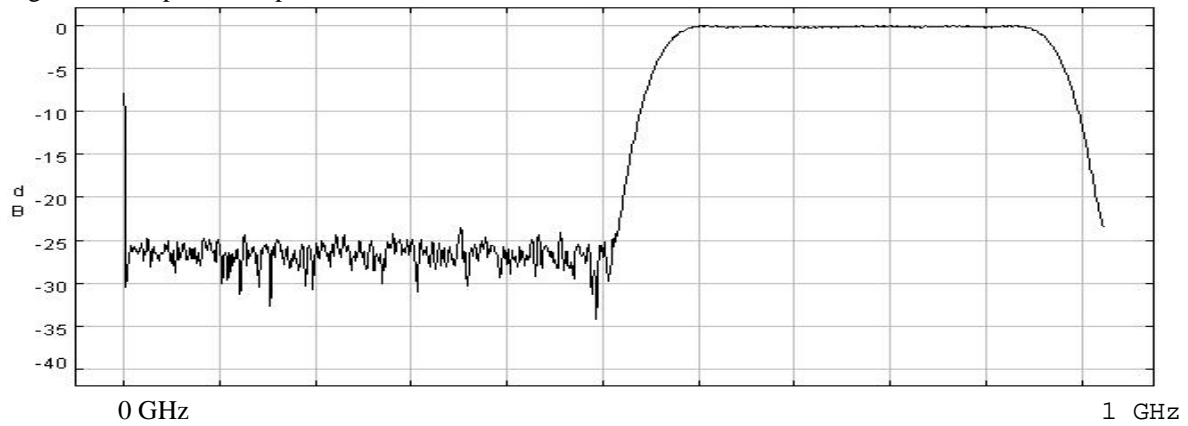


Fig. 6A. 1/4 band filter design with 0.95 band efficiency.

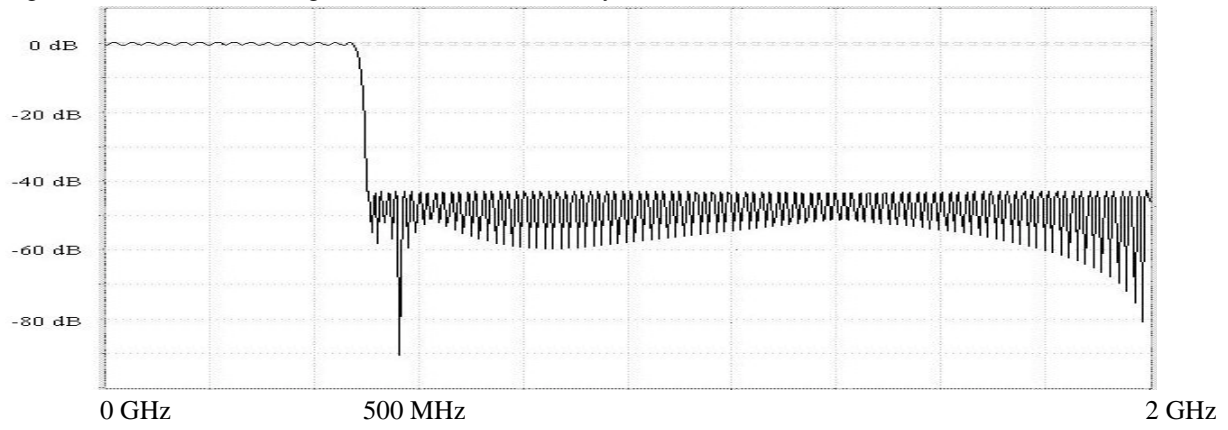


Fig. 6B. 1/4 band filter performance.

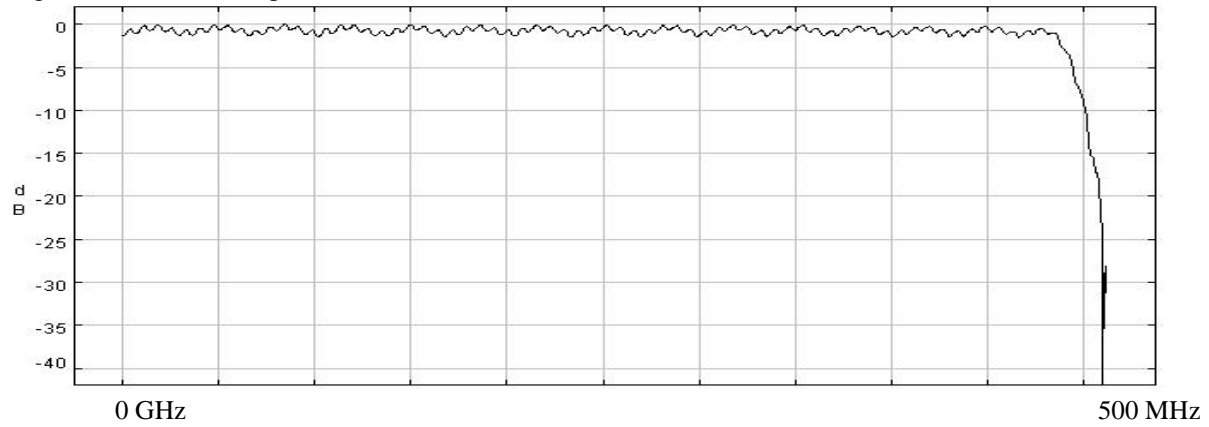


Fig. 7A. 1/4 band filter design with 0.9 band efficiency.

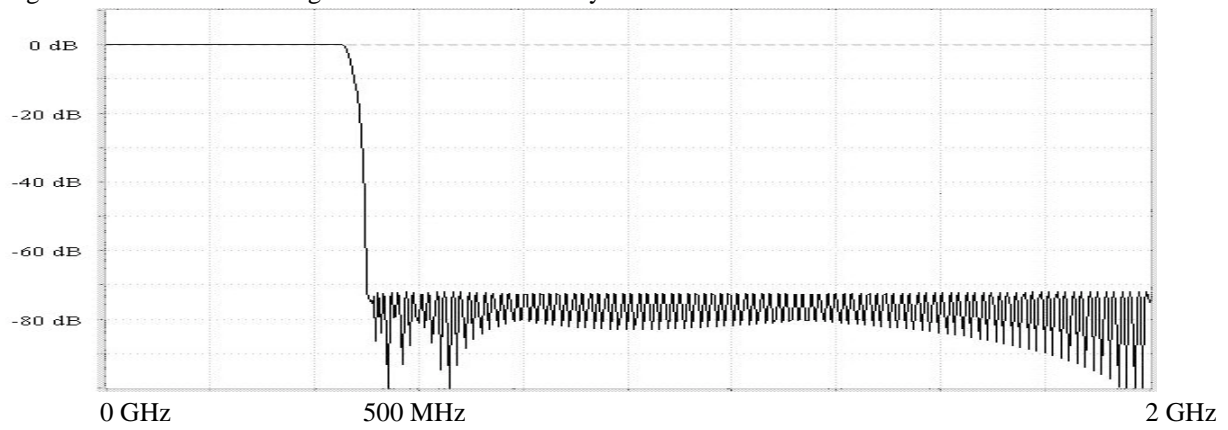


Fig. 7B. 1/4 band filter performance.

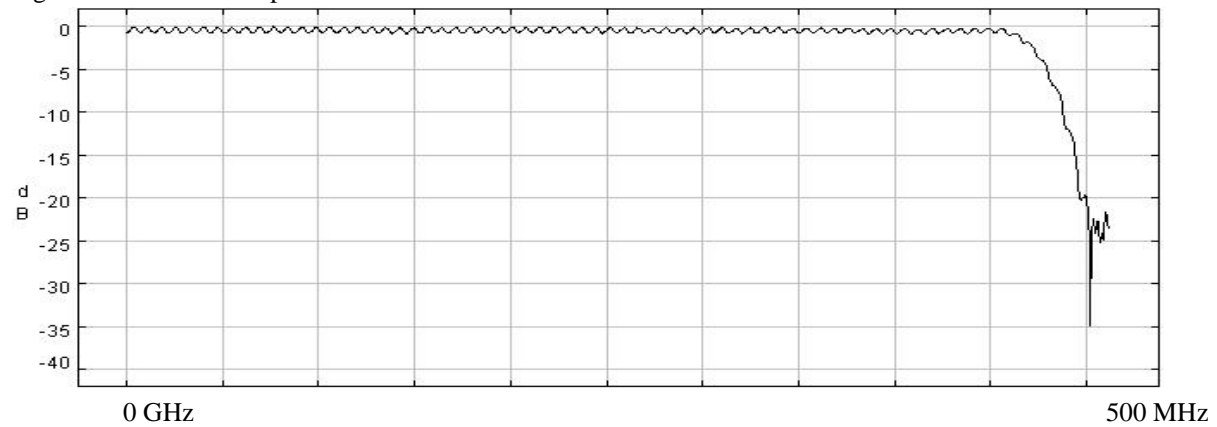


Fig. 8A. 1/4 band filter design with 0.75 band efficiency.

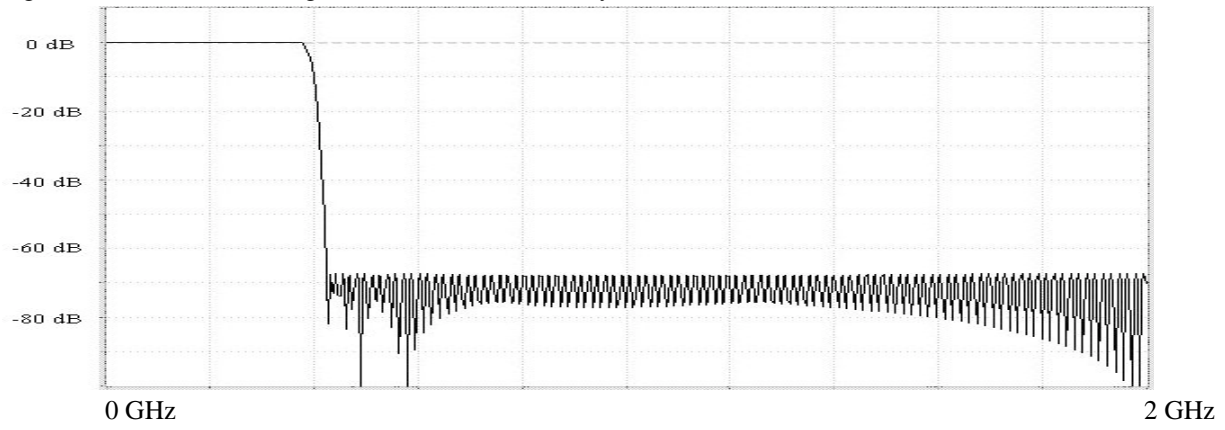


Fig. 8B. 1/4 band filter performance.

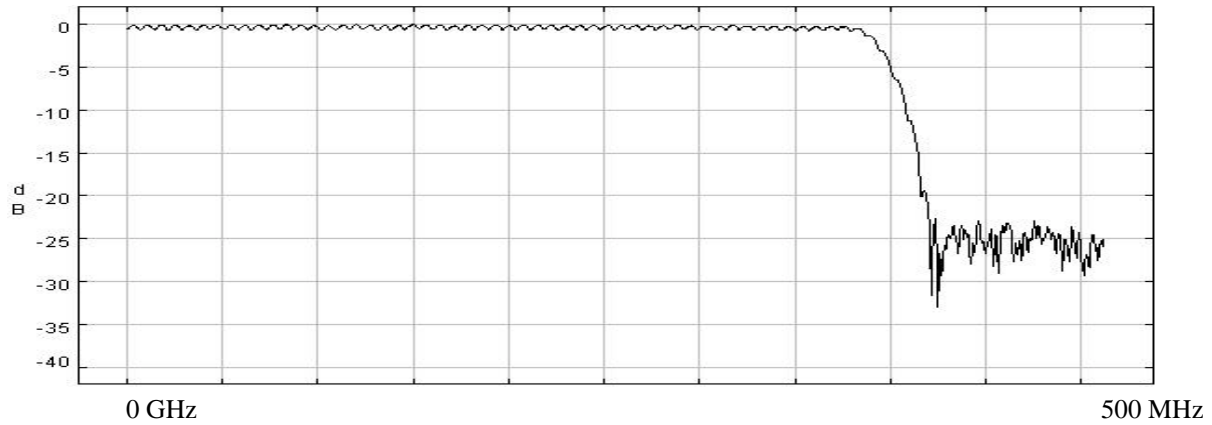


Fig. 9A. 1/4 band filter design (band pass).

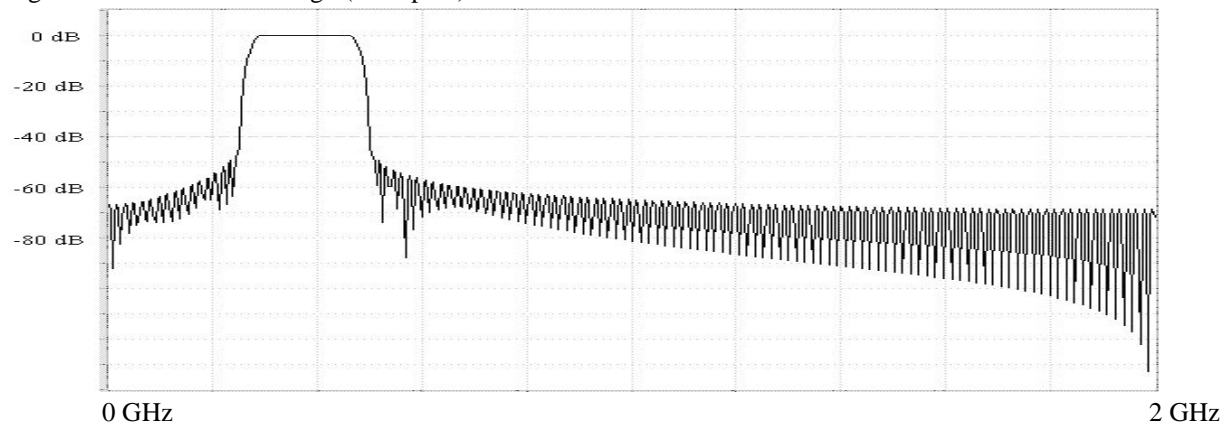


Fig. 9B. Bandpass filter performance.

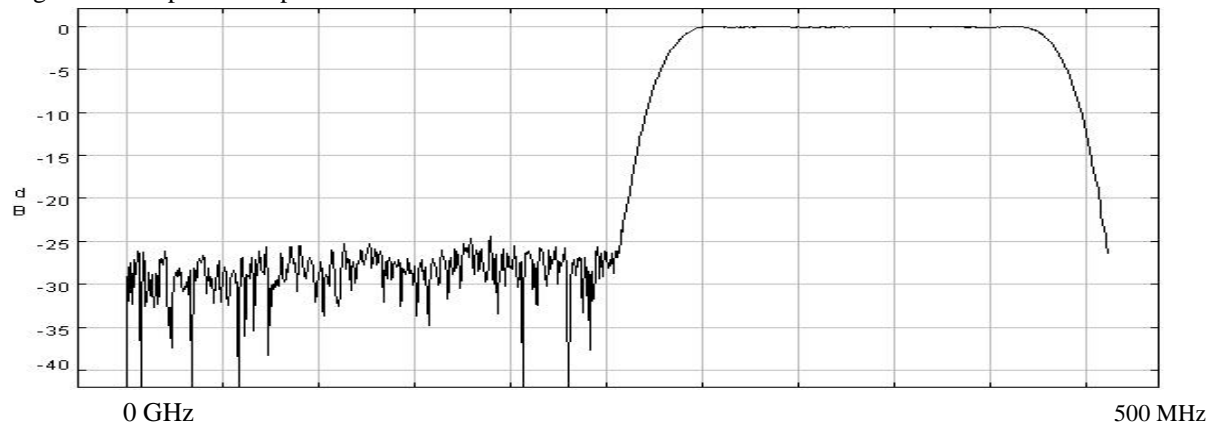


Fig. 10A. 1/8 band filter design with 0.95 band efficiency.

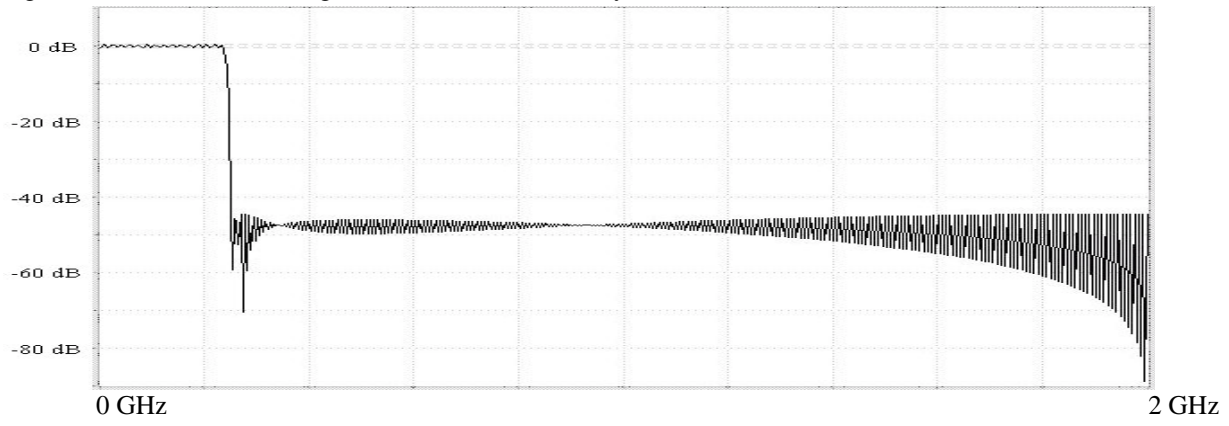


Fig. 10B. 1/8 band filter performance.

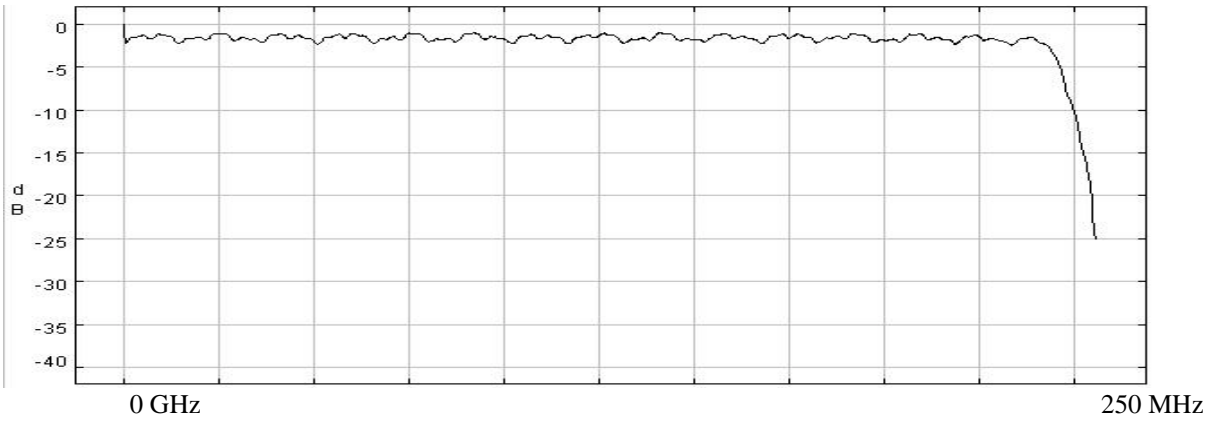


Fig. 11A. 1/8 band filter design with 0.9 band efficiency.

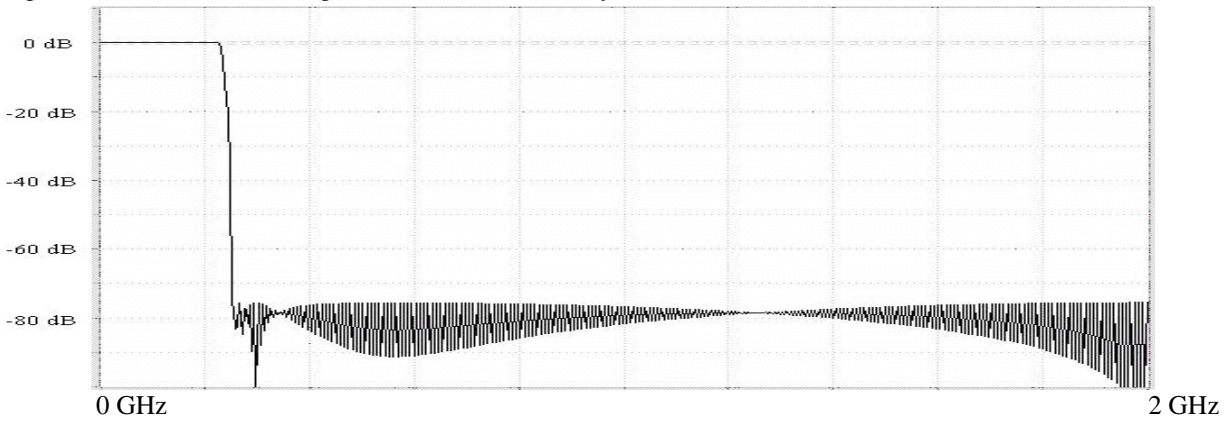


Fig. 11B. 1/8 band filter performance.

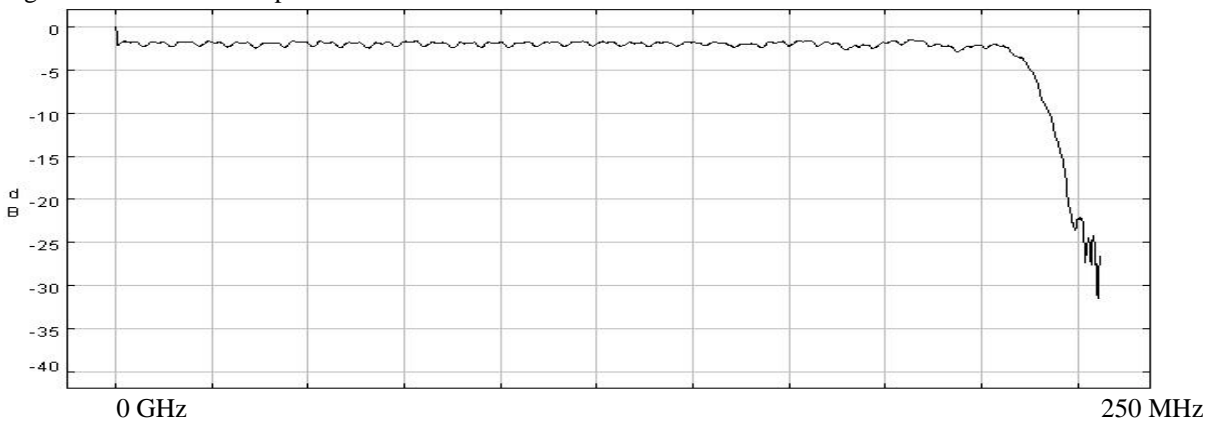


Fig. 12A. 1/8 band filter design with 0.75 band efficiency.

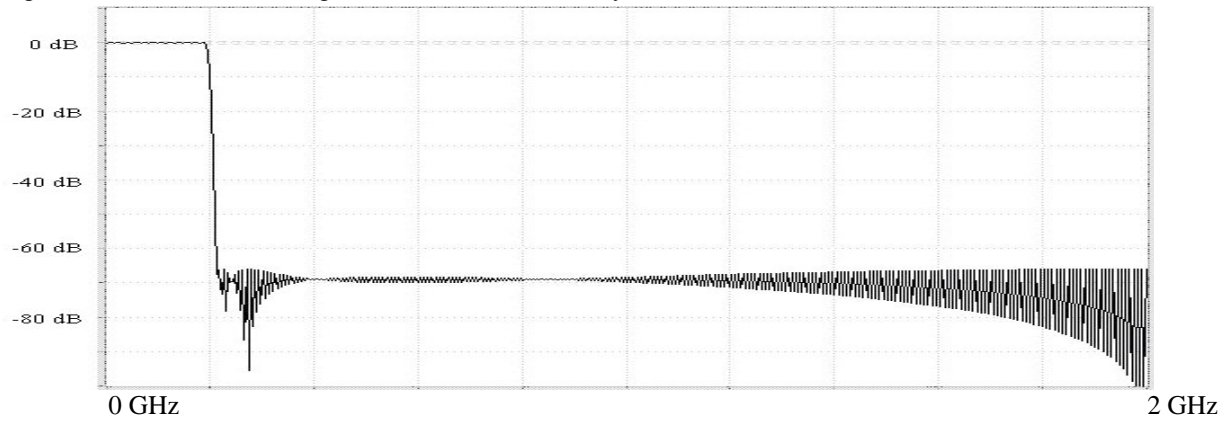


Fig. 12B. 1/8 band filter performance.

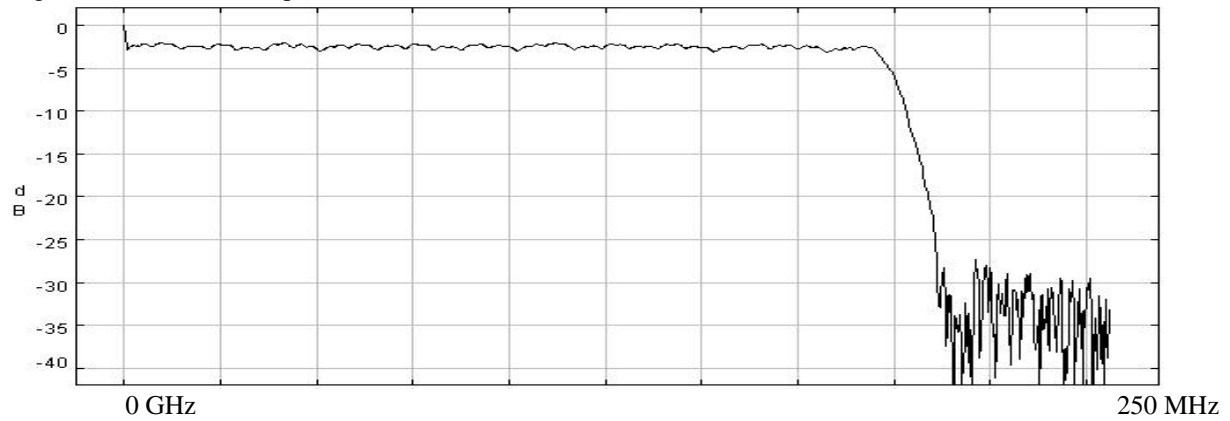


Fig. 13A. 1/8 band filter design (band pass).

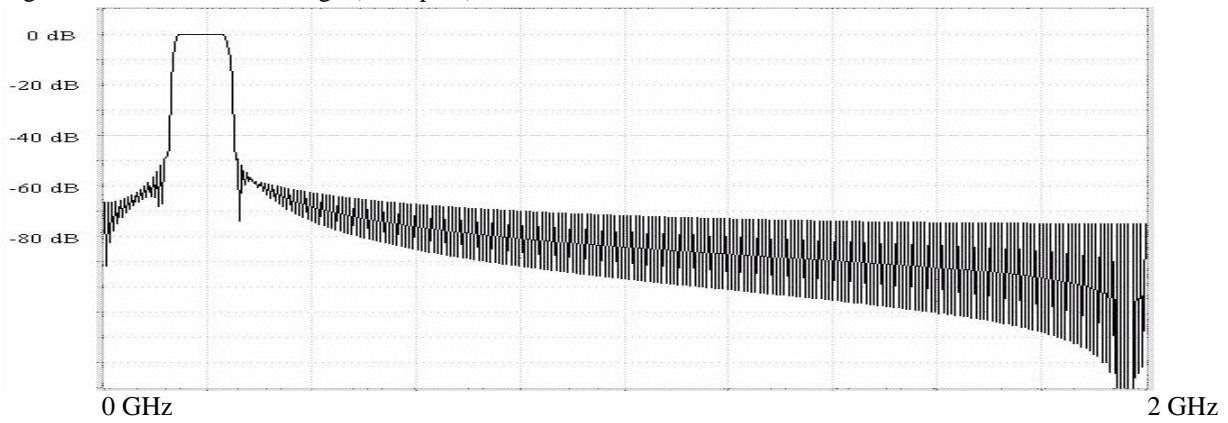


Fig. 13B. Bandpass filter performance.

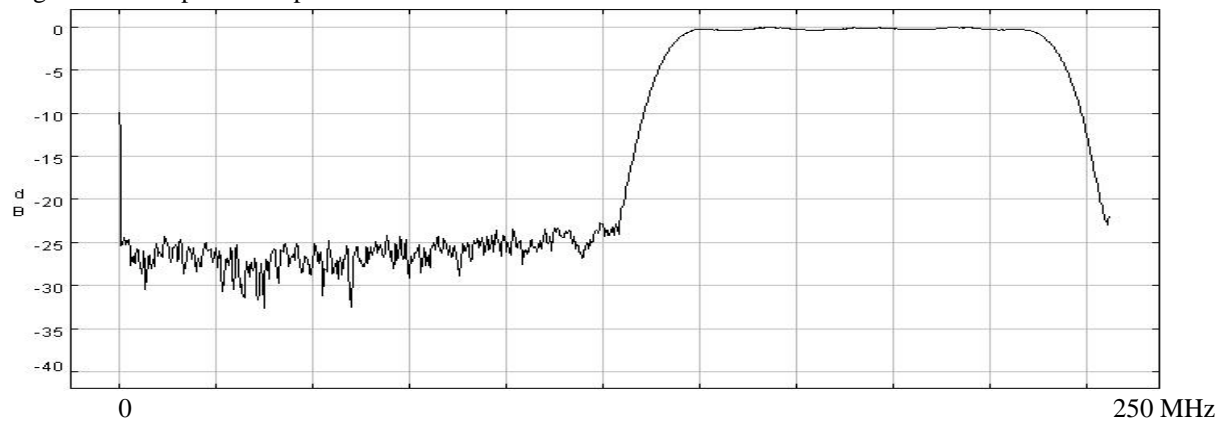


Fig. 14A. 1/16 band filter design with 0.95 band efficiency.

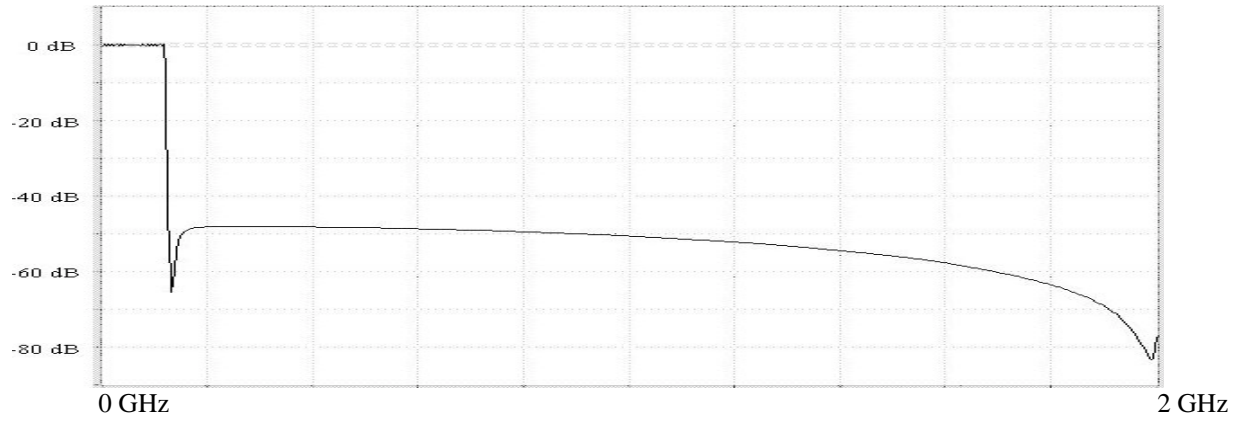


Fig. 14B. 1/16 band filter performance.

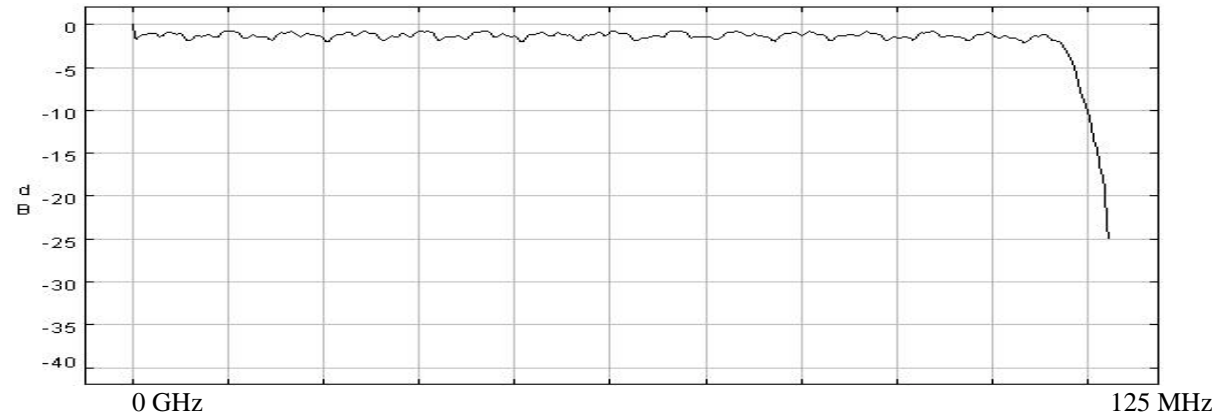


Fig. 15A. 1/16 band filter design with 0.9 band efficiency.

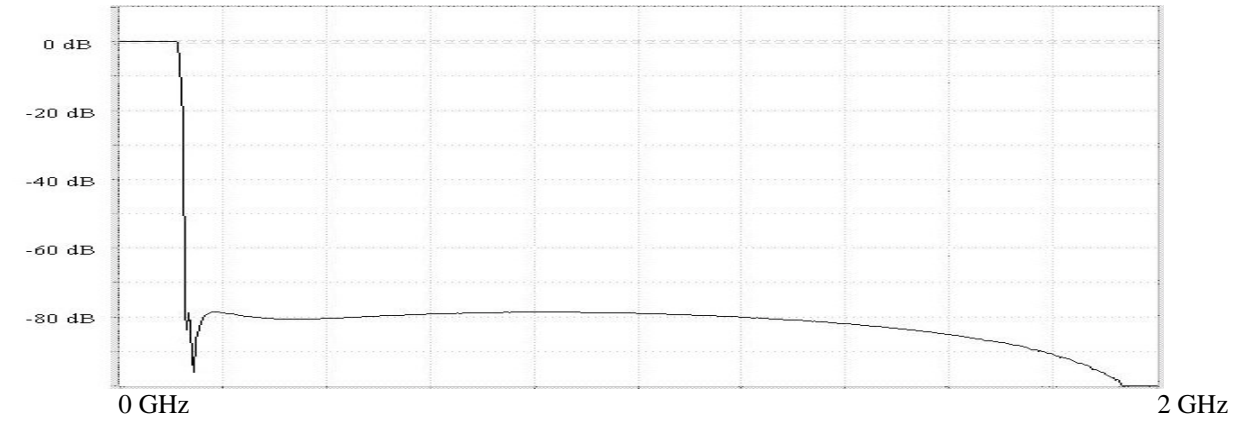


Fig. 15B. 1/16 band filter performance.

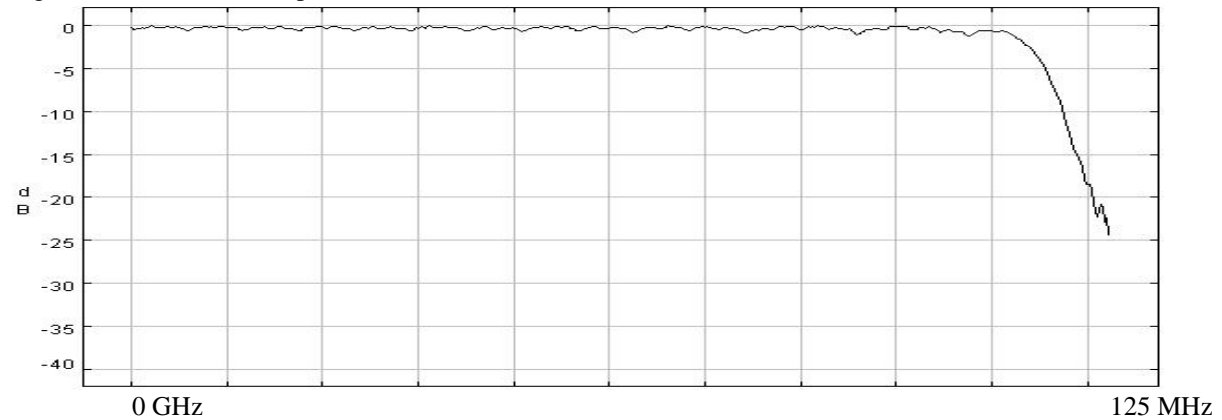


Fig. 16A. 1/16 band filter design with 0.75 band efficiency.

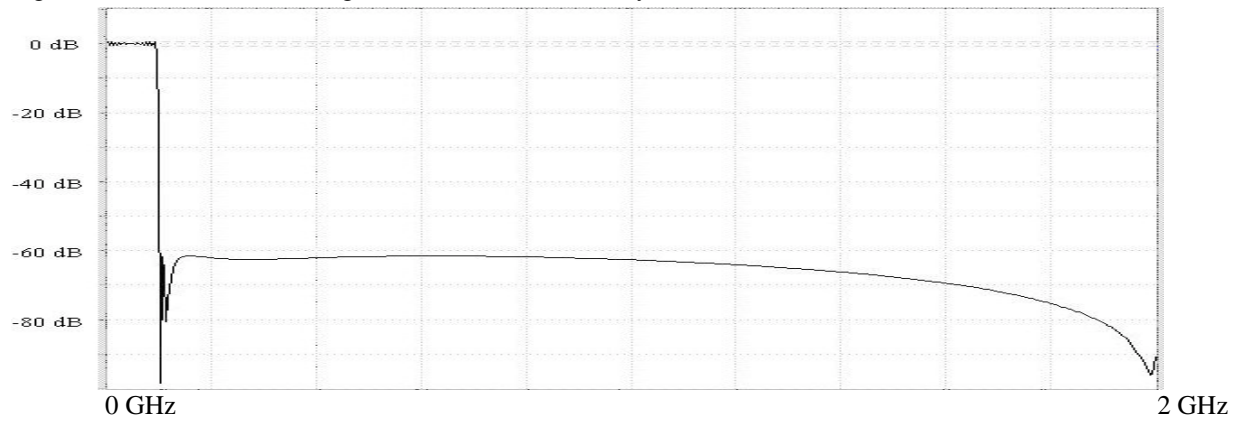


Fig. 16B. 1/16 band filter performance.

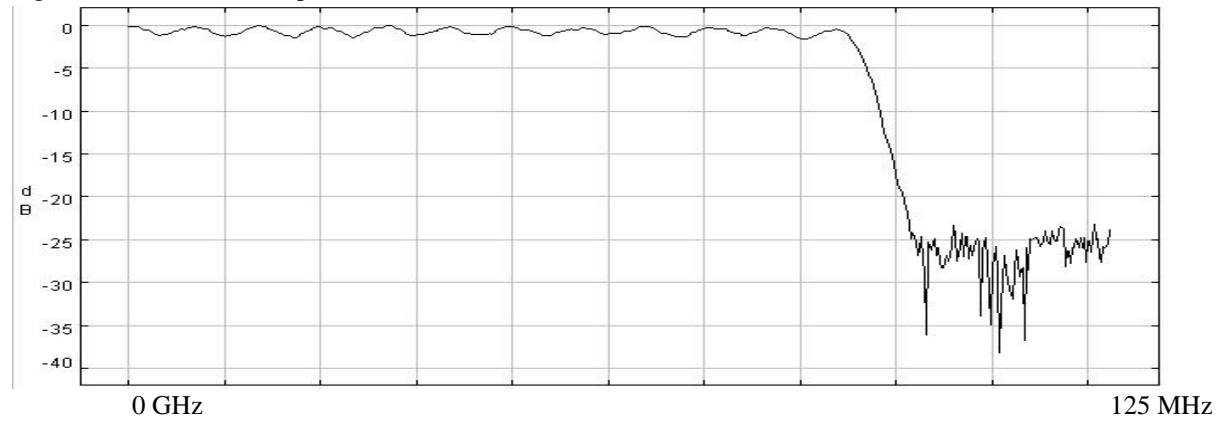


Fig. 17A. 1/16 band filter design (band pass).

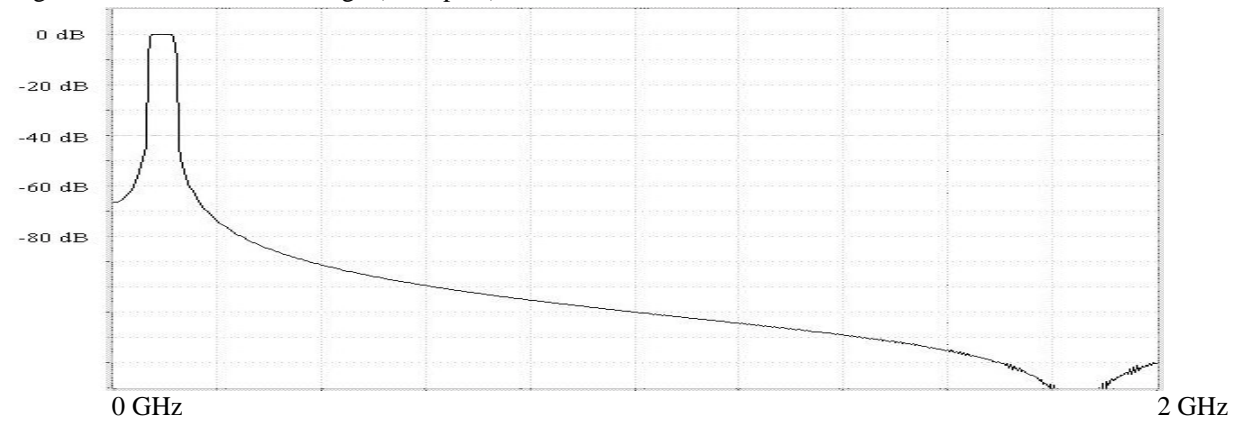


Fig. 17B. Bandpass filter performance.

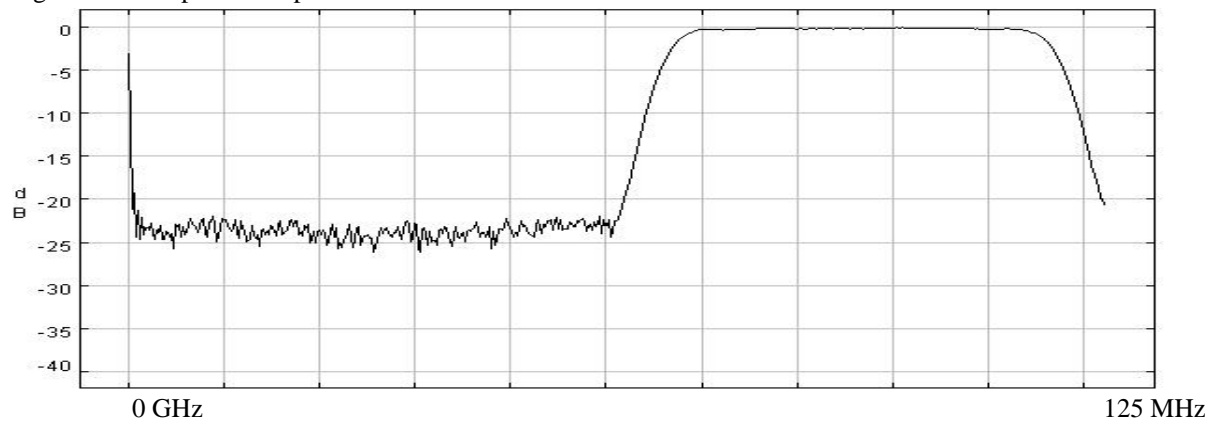


Fig. 18A. 1/32 band filter design with 0.95 band efficiency.

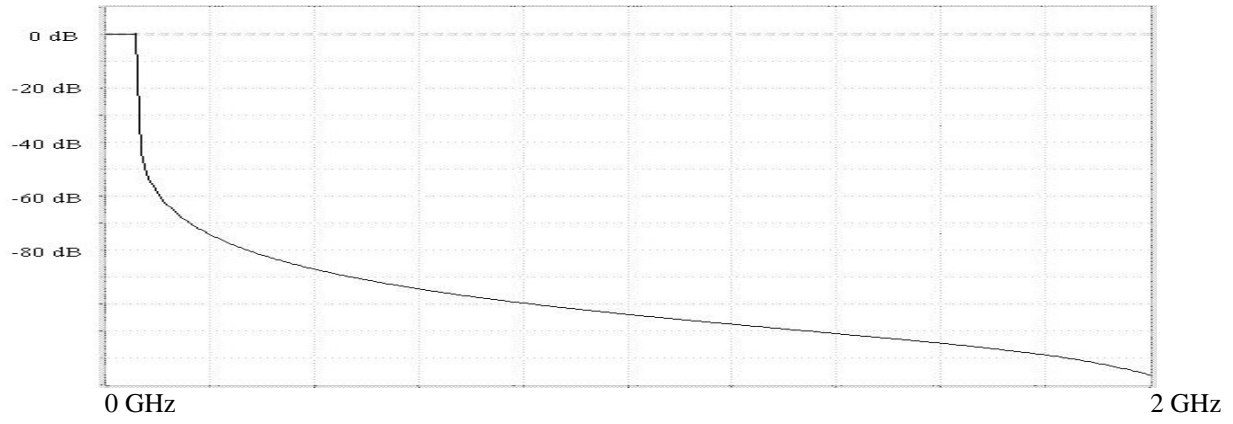


Fig. 18B. 1/32 band filter performance.

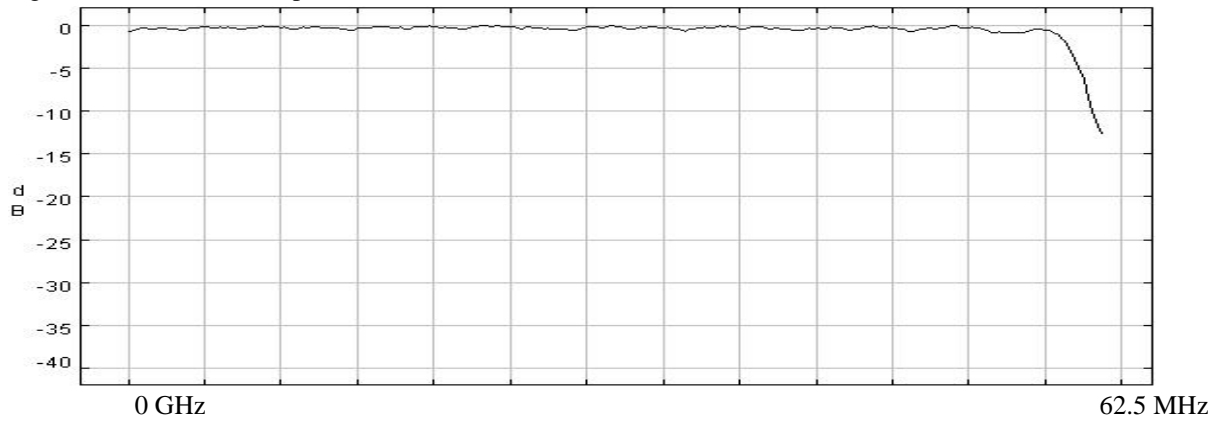


Fig. 19A. 1/32 band filter design with 0.9 band efficiency.

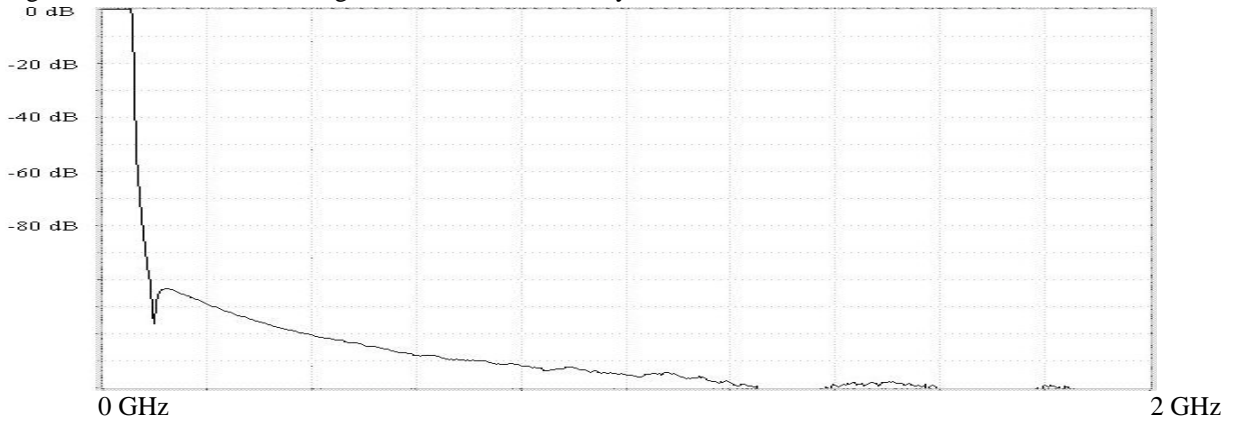


Fig. 19B. 1/32 band filter performance.

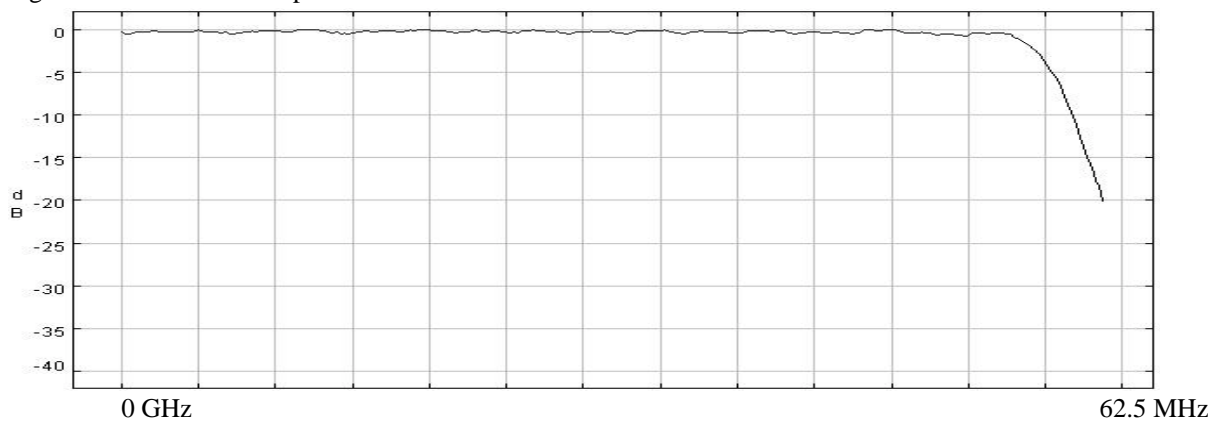


Fig. 20A. 1/32 band filter design with 0.75 band efficiency.

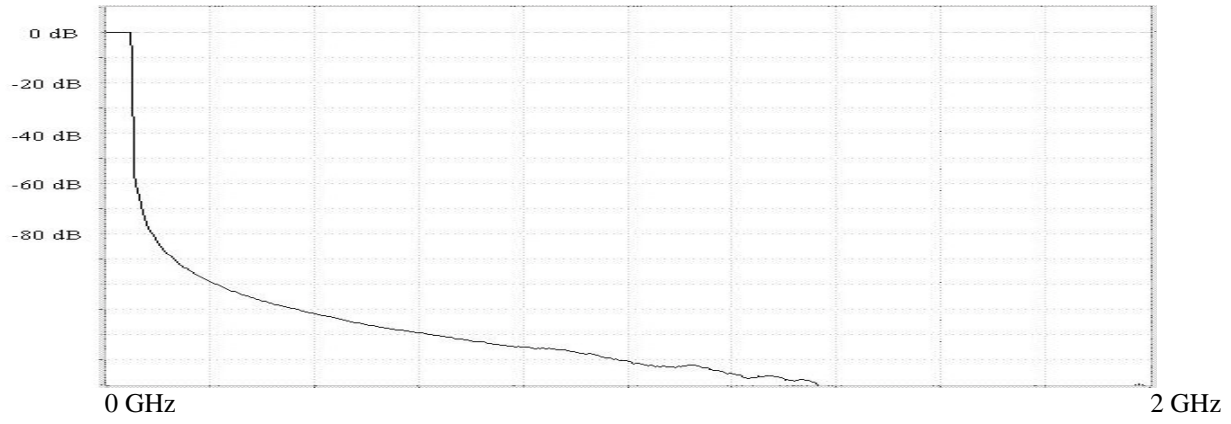


Fig. 20B. 1/32 band filter performance.

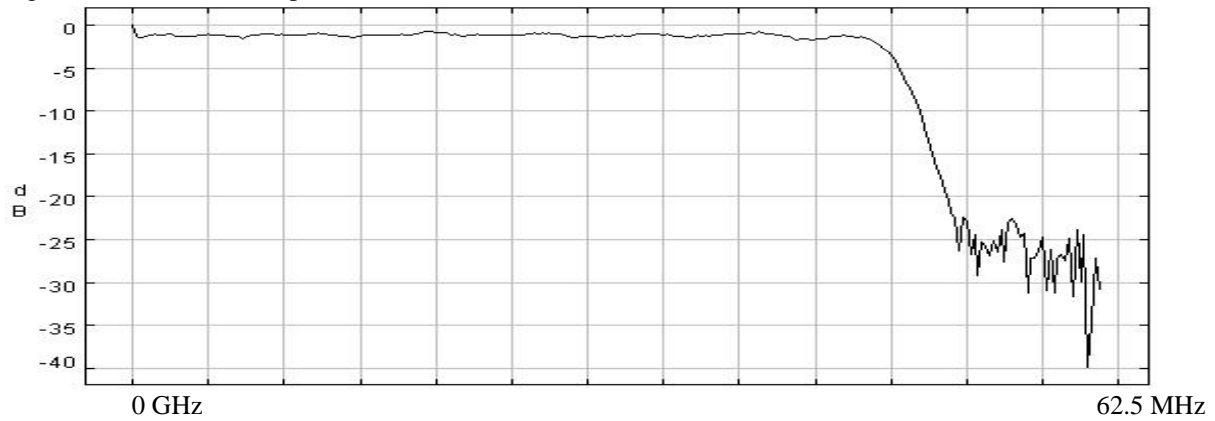


Fig. 21A. 1/32 band filter design (band pass).

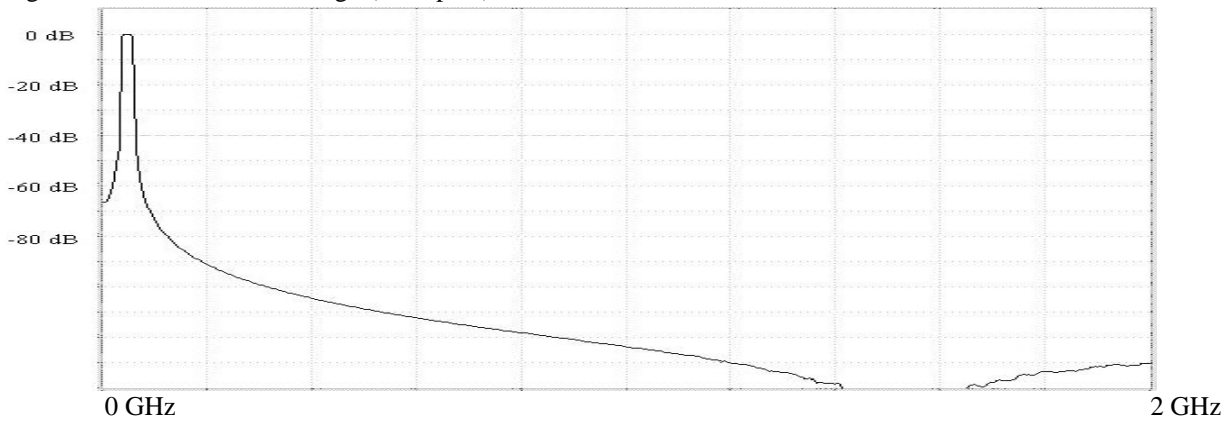
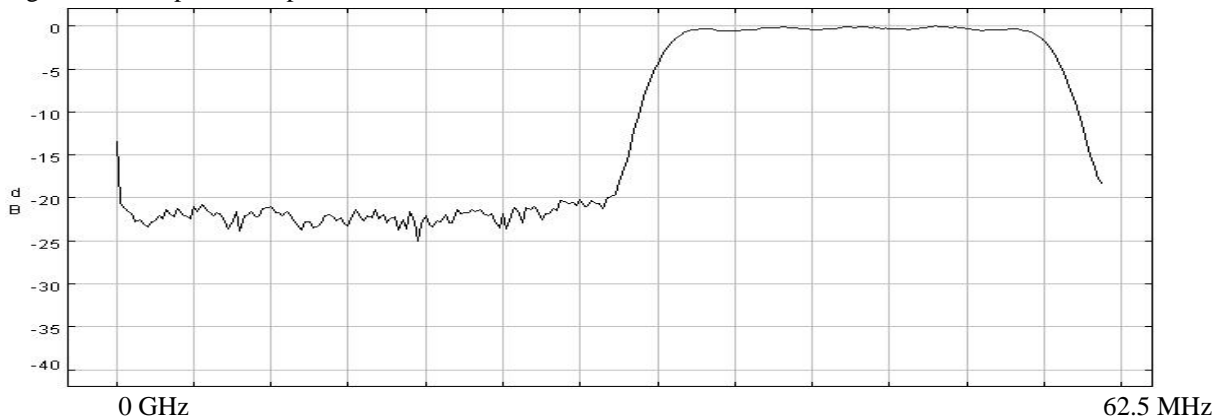


Fig. 21B. Bandpass filter performance.



## STOP BAND TESTING

Stop band performance testing of the prototype digital filter card was done using a (signal-reference)/reference technique. In these tests, "signal" consisted of a wideband continuum component provided by the test fixture PN generator, plus two narrow spectral lines placed in the filter stop band generated by the test fixture NCOs (see Figure 1). "Reference" was provided by the continuum PN generator alone (the NCOs turned off).

By integrating the auto correlation spectrum of the filter card output long enough using alternate signal and reference inputs, attenuation levels of the stop band tones could be measured from the spectral plots of (S-R)/R. Because of inefficiencies in the test fixture involving filling and reading the test fixture RAM buffers, a time limit had to be put on integration time. In all of the results given below, (S-R)/S integrations of the equivalent of 1000 seconds at 4 GS/S were made requiring about 2.5 days test fixture run time each.

In order to perform the (S-R)/R tests described here, much work had to be done on the simulated signal source for the tests. The initial simple 35-bit PN generator plus NCO tones described in earlier reports did not allow the (S-R)/R to "integrate down" as expected, and a noise floor was observed at about -25 dB obscuring the residual stop band tones to be measured.

Two additional stages of randomization in the simulated continuum source had to be provided to prevent systematic effects from masking the stop band tones being measured. The first required the use of 16 PN generators, each of different length, to obtain a 16-bit random signal to "sample." The second randomization element used small RAMs in the test fixture programmed with random numbers between the PN generators and the "sampler" (the random PN numbers looked up random contents in the RAMs).

Stop band rejection was measured using both 4-bit and 3-bit sampling at the filter card input. With every filter tested, no more than 3 dB poorer performance in the out-of-band rejection was observed when using 3-bit samples.

Three filters were tested for stop band rejection: 1/2 band, 1/8 band, and 1/16 band (using 0.95 band efficiency filter designs). (The extreme narrow 1/32 band filter for ALMA applications could not be tested because the test fixture input RAM buffer was not large enough.)

Figures 22 through 27 show the results of (S-R)/R tests run on the prototype filter card. Table 1 below summarizes the stop band rejection test results of these figures. (All plots in Figures 22 through 25 are 1024-point spectra, and plots for Figures 26 and 27 for the 1/16 band filter are 512-point plots. This is because the test fixture input RAM buffer was not large enough to support the full GBT correlator chip 1024-bit lag generator in 1/16 band operation.)

TABLE 1

Figure	Filter	Samples	Aliased Line Position		Stop Band Attenuation	
			Line 1	Line 2	Line 1	Line 2
22	1/2 band	4-bit	point 654	point 932	> 35 dB	33 dB
23	1/2 band	3-bit	point 654	point 932	> 35 dB	30 dB
24	1/8 band	4-bit	point 274	point 836	> 45 dB	42 dB
25	1/8 band	3-bit	point 274	point 836	> 45 dB	40 dB
26	1/16 band	4-bit	point 352	point 267	> 45 dB	35 dB
27	1/16 band	3-bit	point 352	point 267	> 45 dB	35 dB

Table 1 shows the digital filter performance with the prototype filter card programmed as a 1/2 band, a 1/8 band, and a 1/16 band filter. Each filter type was tested using both 4-bit and 3-bit samples. Two spectral lines produced by the test fixture NCOs were placed in the stop band of the filters being tested. Table 1 shows the spectral point number in the (S-R)/R spectrum that the two lines were expected to alias to considering the 1024- or 512-point spectra.

In every case, one of the two lines was below the noise floor, and only a minimum attenuation level could be stated. In the 1/2 band filter and the 1/8 band filter, a line aliased to the 90% and 81% point, respectively, of the maximum pass band frequency, and the filter attenuation at this point in the spectrum could be measured.

A systematic noise floor can be seen emerging in the 1/16 band plots indicating that the continuum noise source is still not random enough for these measurements.

Zero dB references for the attenuation measurements above were obtained from (S-R)/R plots in which the NCO signals were in-band, but with the same power level as the out-of-band runs.

Fig. 22. (signal-reference)/reference result of 1/2 band filter with 4-bit sampling.

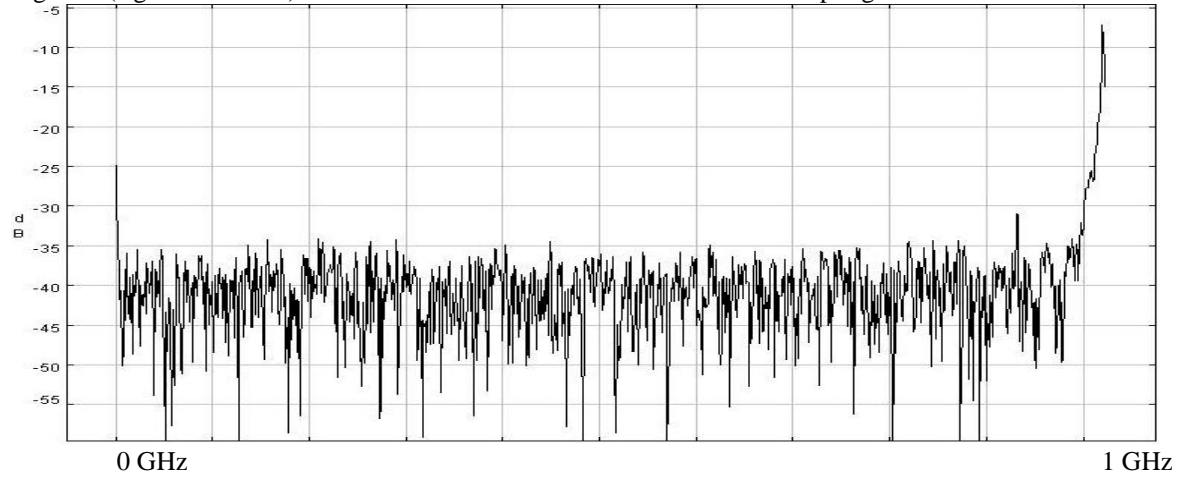


Fig. 23. (signal-reference)/reference result of 1/2 band filter with 3-bit sampling.

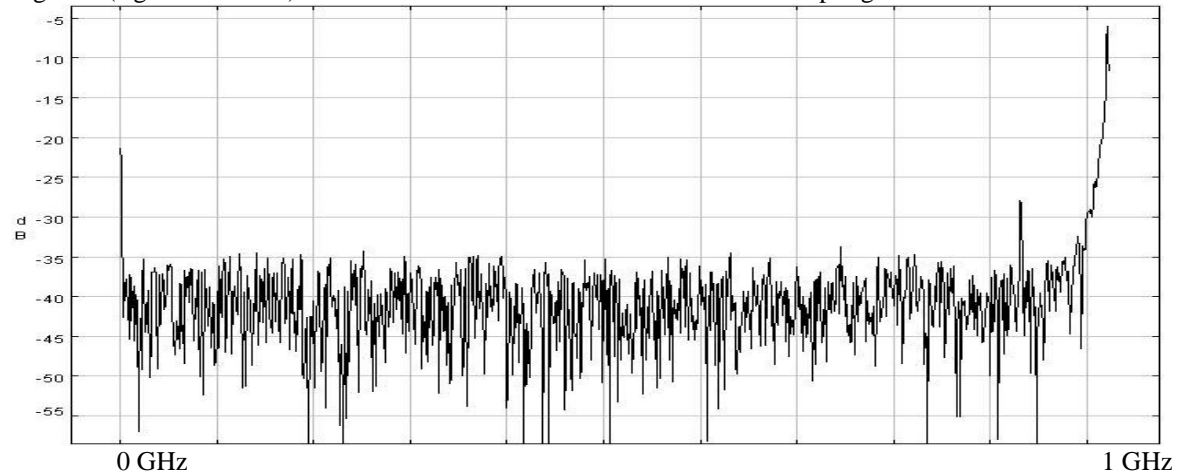


Fig. 24. (signal-reference)/reference result of 1/8 band filter with 4-bit sampling.

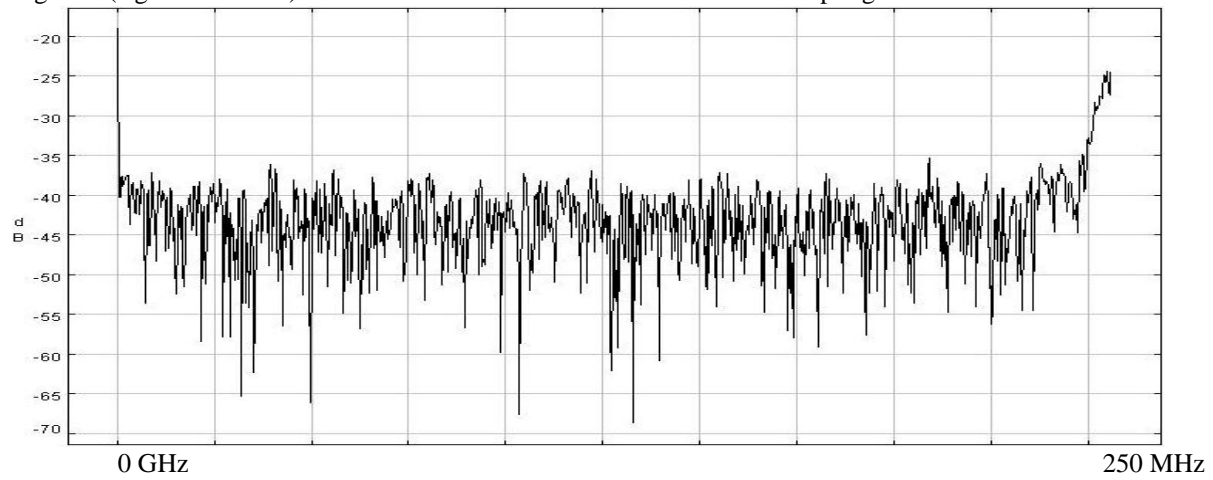


Fig. 25. (signal-reference)/reference result of 1/8 band filter with 3-bit sampling.

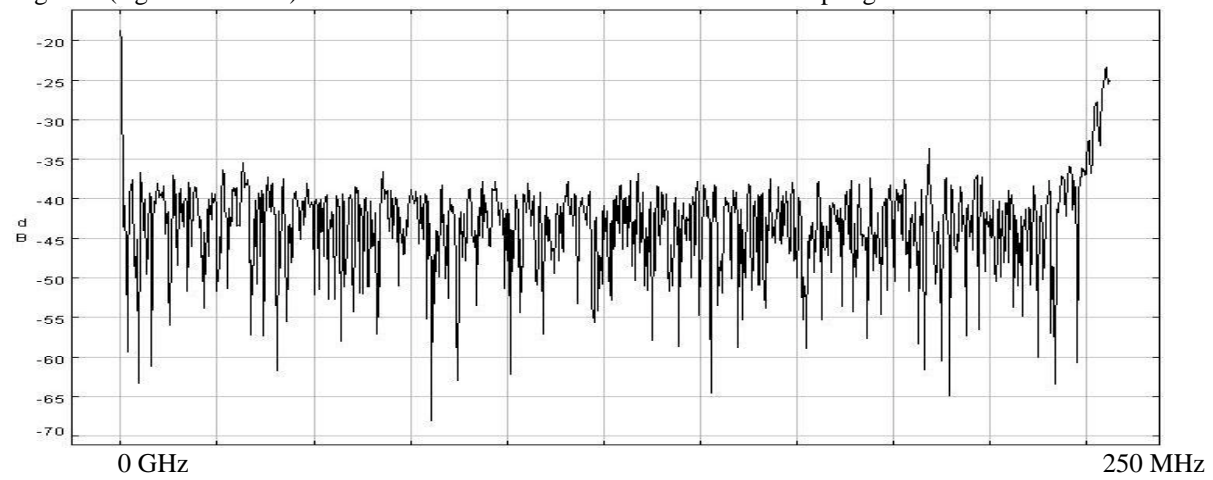


Fig. 26. (signal-reference)/reference result of 1/16 band filter with 4-bit sampling.

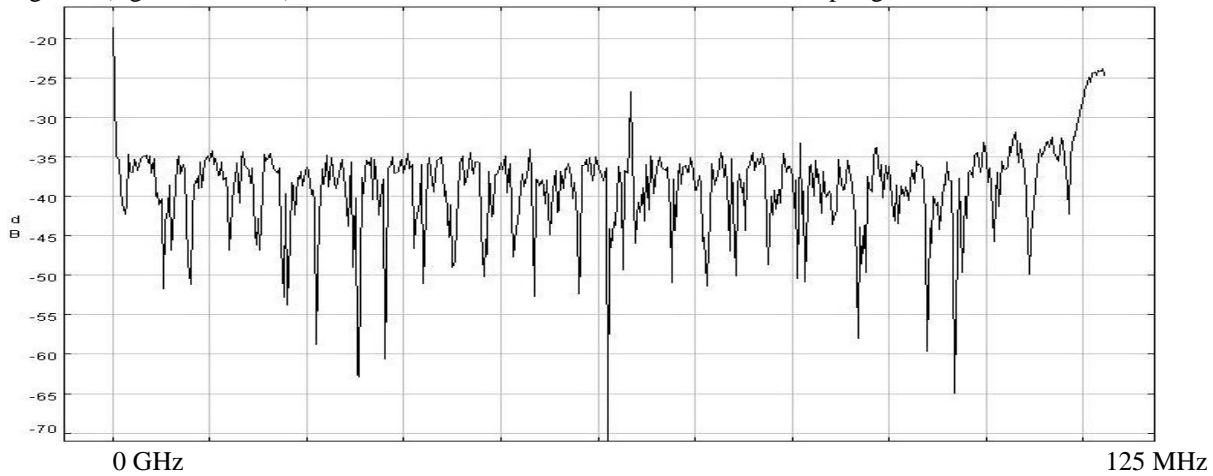
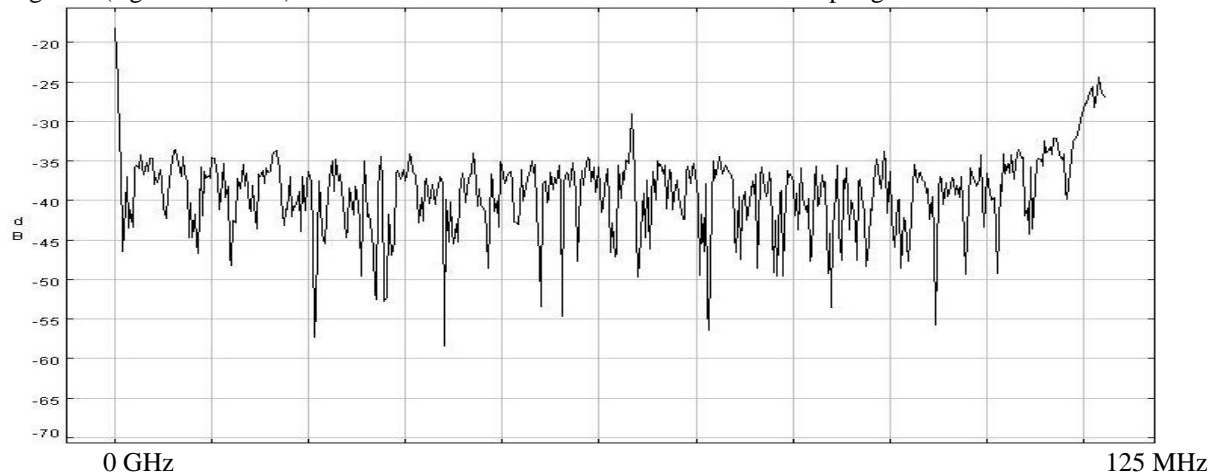


Fig. 27. (signal-reference)/reference result of 1/16 band filter with 3-bit sampling.



## FILTER CARD POWER DISSIPATION

One point of concern with the filter card design is the high card power requirement. With 4-bit samples and the full 125 MHz clock rate, the filter card dissipates 55.3 watts when programmed as a 1/2 band filter. Programming the filter for more narrow bandwidths reduced the power requirement, so the 1/2 band configuration is the worst case. Operating the card with 3-bit samples reduces the power requirement by about 7%.

While a card dissipation in the 50-watt level is not of concern, most of the power in the filter card is dissipated in just 8 chips, the tap weight multiplier chips. These chips dissipated about 5 watts each.

One technique investigated to reduce the power requirement of the filter card was to add small numerical offsets to the tap weight look-up tables. The idea was that the result of most of the tap weight multiplications would be small, and bipolar samples would result in frequent sign changes. With small numbers, frequent sign changes mean that there would be a large number in flip-flop logic transitions per unit time since the numbers were essentially all extended sign bits expressed in 2's complement arithmetic. Many logic level transitions per unit time imply a high power dissipation in CMOS chips.

Small offsets added to these small tap weight multiplication results meant that they would be unipolar most of the time and, since they were expected to be small, no loss of dynamic range in the filter would result. With small unipolar results, only a few flip-flop stages could be expected to change from clock to clock.

Offsets were selected such that they canceled out after the first five stages in the filter card adder tree. This technique was tried in the prototype filter card and resulted in a power savings of about 14%. All of the tests with results given in Figures 22 through 27 were performed using the tap weight offsets to prove that there was no degeneration in filter performance.